Geomechanics and Engineering, Vol. 2, No. 1 (2010) 57-69
DOI: http://dx.doi.org/10.12989/gae.2010.2.1.057

Reliability assessment of EPB tunnel-related settlement

Anthony T.C. Goh* and A.M. Hefney

School of Civil & Environmental Engineering, Nanyang Technological University, Nanyang Avenue, Singapore 639897

(Received October 30, 2009, Accepted March 15, 2010)

Abstract. A major consideration in the design of tunnels in urban areas is the prediction of the ground movements and surface settlements associated with the tunneling operations. Excessive ground movements can damage adjacent building and utilities. In this paper, a neural network model is used to predict the maximum surface settlement, based on instrumented results from three separate EPB tunneling projects in Singapore. This paper demonstrates that by coupling the trained neural network model to a spreadsheet optimization technique, the reliability assessment of the settlement serviceability limit state can be carried out using the first-order reliability method. With this method, it is possible to carry out sensitivity studies to examine the effect of the level of uncertainty of each parameter uncertainty on the probability that the serviceability limit state has been exceeded.

Keywords: first-order reliability method; limit state surface; neural networks; reliability; settlement; tunnel.

1. Introduction

Ground movements and surface settlements associated with tunnel operations are a major concern in the design of tunnels in urban areas as excessive movements can damage nearby buildings and utilities. Various procedures are available to estimate the ground surface settlement including the use of empirical equations (Attewell 1977, Mair *et al.* 1993), simple equations based on the theory of elasticity (Uriel and Sagaseta 1989) or numerical tools such as the finite element method (Rowe and Lee 1992). Neural networks (NN) have also been used successfully for predicting the maximum surface settlement in a number of tunneling projects (Shi *et al.* 1998, Kim *et al.* 2001, Suwansawat and Einstein 2006, Santos and Celestino 2008). In all these projects, the neural networks were trained and tested using instrumented data and data from the tunnel operational parameters and the geological parameters.

To prevent or minimize damage to nearby structures involves the assessment of the serviceability limit state. Typically this involves setting a limiting value on the maximum tolerable surface settlement (based on acceptable movement of the nearby structures) and ensuring that the calculated settlement using the methods described above is not exceeded. Because of the uncertainties in the tunnel operational and geological parameters (e.g., soil properties, tunnel advance rate, and tunnel

*Corresponding author, Associate Professor, Ph.D., E-mail: ctcgoh@ntu.edu.sg

face pressure), a probabilistic approach is presented herein to assess the reliability of the serviceability limit state. Reliability analysis allows one to more systematically treat uncertainties.

Since the ground settlement from EPB tunnel operations is a complicated and nonlinear problem, the serviceability limit state surface is difficult to determine explicitly in terms of the random variables. In this paper, the serviceability limit state is derived from a neural network algorithm. The data for training and testing the neural network model were obtained from measured maximum surface settlements resulting from earth pressure balance (EPB) tunneling machines for three separate projects in Singapore. The trained neural network model is then coupled with the first-order reliability method through a spreadsheet optimization technique to determine the reliability index.

The fundamental concepts of neural networks are introduced in the following section. The subsequent two sections then outline the ground conditions for the three projects and the use of the neural network to model the surface settlement and serviceability limit state. This is followed by a description of basic reliability concepts and the use of the neural network model to assess the reliability of the surface settlement predictions.

2. Overview of neural networks

The neural network is composed of simple inter-connected nodes or neurons as shown in Fig. 1. The neuron connections have weights that are adapted (trained) to improve its overall performance. In the back-propagation neural network, the neurons are arranged in layers and are connected so that the neurons in a layer receive inputs from the preceding layer and send out outputs to the following layer (Rumelhart *et al.* 1986). External inputs are applied at the first layer and system outputs are taken at the last layer. The intermediate layers are called hidden layers.

For this EPB tunnel settlement problem, the neural network inputs are geotechnical properties and

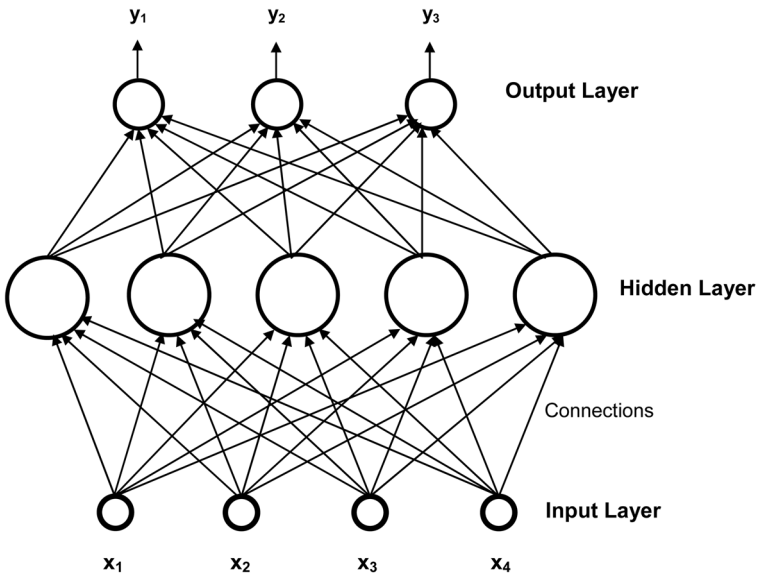

Fig. 1 Typical neural network architecture comprising 4 input neurons, 5 hidden neurons and 3 output neurons

tunnel operational factors such as the tunnel advance rate and tunnel face pressure. The neural network output is the maximum surface settlement.

The basic concepts of the back-propagation algorithm can be found in the literature (Rumelhart *et al*. 1986, Caudill and Butler 1991). Back-propagation neural networks are trained by feeding a series of examples of associated input and target (desired) output values. Each hidden and output unit processes its inputs by multiplying each input by its weight, summing the product, and then processing the sum using a non-linear transfer function to produce a result. The sigmoid (logistic) function is commonly used as the transfer function.

The general objective of "training" the neural network is to modify the connection weights to reduce the errors between the actual output values (measured surface settlement) and the target output values (predicted surface settlement) to a satisfactory level. This process is carried out through the minimization (optimization) of the defined error function using the gradient descent approach. The sum squared error function is commonly adopted as the error function. After convergence occurs (i.e., the errors are minimal), the associated trained weights of the model are tested with a separate set of "testing" data that was never used in training the neural network. This testing is used to assess the generalization capability of the trained neural network model to produce the correct input-output mapping, even when the input is different from the examples used to train the network. The determination of the optimal number of hidden neurons in the network architecture is usually carried out by trial-and-error; the usual approach is to begin with a small number of hidden neurons and train the network, iteratively repeating the process of increasing the number of hidden neurons until no further improvement in the network performance is obtained.

A single hidden layer of the back-propagation has been proven to be capable of providing accurate approximations to any continuous function provided there are sufficient hidden neurons (Hornik 1991). The hidden neurons play a crucial role in the neural network learning by progressively "discovering" the salient features that characterize the training data. They do so by performing a nonlinear transformation on the input data into a new space called the hidden space. In a sense, the "training" of the neural network may be viewed as a curve-fitting (approximation) problem in high-dimensional space. There are two advantages of using neural networks to model the nonlinear limit state surface: (a) in the neural network approach, it is not necessary to know the underlying relationship between the input variables and the output unlike the polynomial regression modeling technique, and (b) the neural network approach generally outperforms most mathematical regression models in terms of the modeling accuracy.

At the end of the training phase, the neural network represents a model that should be able to predict the "correct" surface settlement given the input data pattern. Using the optimal trained connection weights, it is possible to develop a mathematical expression relating the input variables and the output variable (predicted surface settlement δ_{NN}). The mathematical relationship to determine δ_{NN} is shown in the Appendix. For a given limiting surface settlement δ_{Lim} the limit state surface can be defined as $G(\mathbf{x}) = \delta_{Lim} - \delta_{NN}$. This expression then can be used for reliability index calculations and is described in a later section.

3. Ground conditions

The major works for the construction of mass rapid transit tunnels in Singapore have been described in a number of publications (Hulme and Burchell 1999, Izumi *et al.* 2000, Shirlaw *et al.*

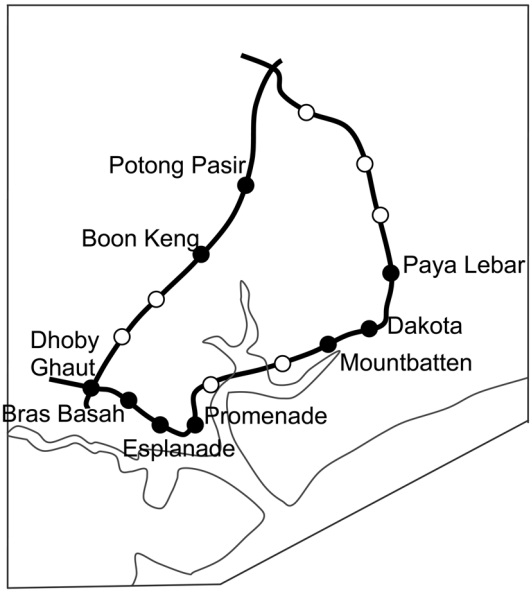

Fig. 2 Map showing project locations

2003). The four major soil types encountered in this study were:

(a) Kallang formation. This is comprised of near-normally consolidated marine clay as well as loose fluvial sands and moderately stiff fluvial clay.
(b) Old Alluvium. This is comprised of mainly dense alluvial silty sands and clays.
(c) Fort Canning Boulder Bed. This is comprised of a colluvial deposit of strong to very strong quartzite boulders in a hard clayey silt matrix.
(d) Jurong formation. This is comprised primarily residual soils of clayey silt and sandy clay of medium plasticity and clayey to silty sand.

The engineering properties of these formations are described in Sharma *et al.* (1999) and Hulme and Burchell (1999).

The tunnel settlement data used in this paper were obtained from three separate mass rapid transit projects in Singapore. The locations of the projects are shown in Fig. 2. Fig. 3 shows the soil profiles of the three projects. Twin-bored tunnel drives using EPB machines were used (Table 1). Precast concrete tunnel linings of 5.8 m internal diameter were used throughout. Surface settlement points were installed at approximately 25 m intervals along the tunnel alignment. A total of 148 settlement patterns were obtained from the three projects.

There are numerous factors that influence the surface settlement. They can be subdivided into three major categories (Suwansawat and Einstein 2006): (1) tunnel geometry, (2) geological conditions and (3) EPB operational factors. Fig. 4 shows the tunnel advance rate AR versus the measured maximum surface settlement as a function of S1 which is the mean SPT N value (standard penetration test) of the soil layers above crown level up to ground surface. Fig. 5 shows plot of the tunnel advance rate AR versus the measured maximum surface settlement as a function of S2 which is the average of the SPT N values at the crown, middle and invert levels. In general while it can be seen that the surface settlements are less than 20 mm for S1 and S2 with N values

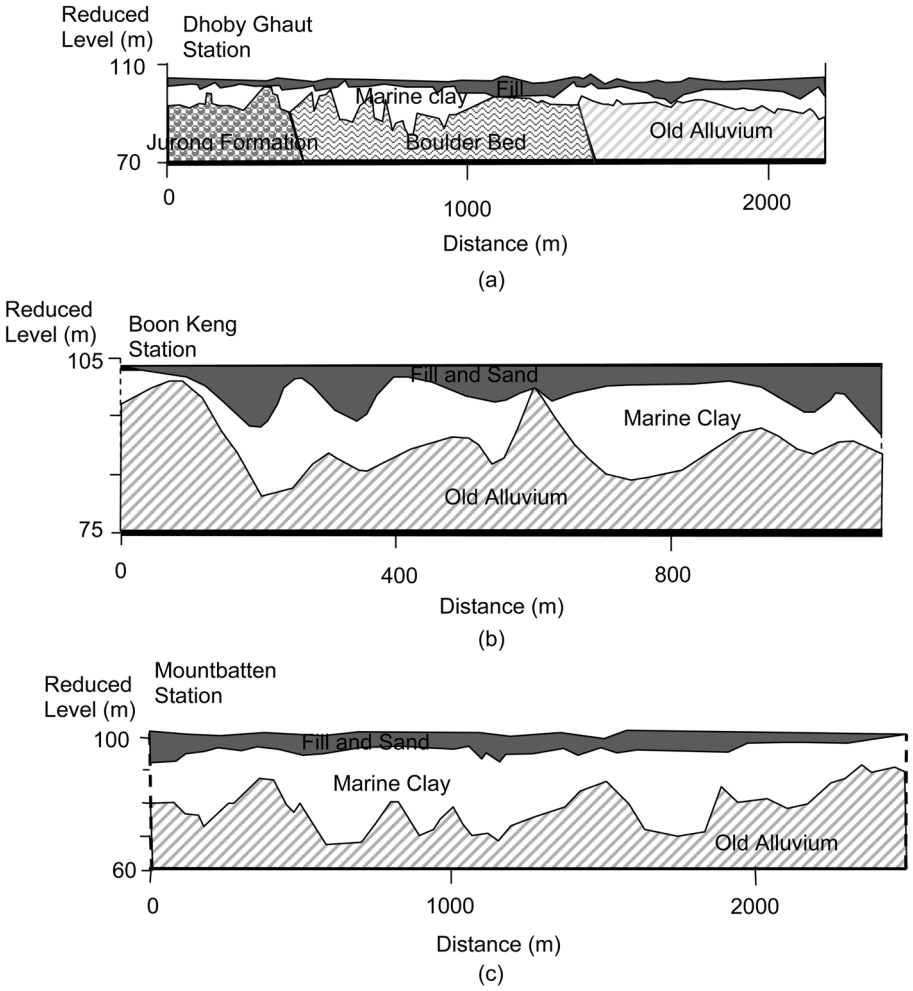

Fig. 3 Longitudinal soil profiles of projects

greater than 30, it is difficult to establish any clear relationship between the surface settlement, the advance rate, S1 and S2. Hence a neural network algorithm was used to determine the relationship between the surface settlement, and the geological and EPB operational factors. As will be shown in the following section, the back-propagation neural network is capable of learning from the training examples and can capture the nonlinear and complex interactions among the various inputs and the surface settlement.

4. Neural network analysis

The NN model used to model the tunnel settlement consisted of eight inputs that represented the tunnel geometry, geological conditions and the EPB operation. The two important geometrical factors that influence the surface settlement are the tunnel diameter and the tunnel depth H

Table 1 Summary of tunnel project details

Contract	C705	C823	C825
TBM manufacturer	Hitachi-Zosen	Hitachi-Zosen	Herrenknecht
Drive length (km)	1.3	3.3	1.5
Tunnel drive (No.)	2	2	2
Outside diameter (m)	6.44	6.63	6.58
Internal diameter (m)	5.8	5.8	5.8
Stations	Boon Keng and Potong Pasir	Mountbatten, Dakota and Paya Lebar	Dhoby Ghaut, Bras Basah, Esplanade and Promenade
Geology (general description)	Mostly Old Alluvium with marine clay	Fill overlying Kallang formation and Old Alluvium	Soft marine clay, Old Alluvium, Fort Canning Boulder bed, Jurong formation

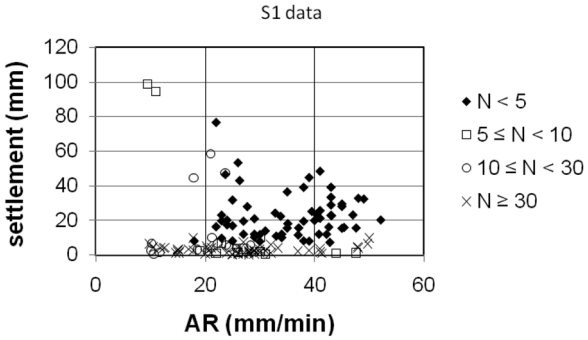

Fig. 4 Relationship between S1, tunnel advance rate and surface settlement

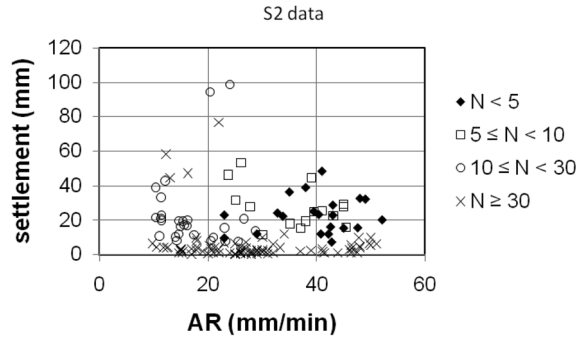

Fig. 5 Relationship between S2, tunnel advance rate and surface settlement

(measured from the tunnel crown to the ground surface). However, since the internal diameter of the tunnels for all three projects were 5.8 m, this parameter was omitted from the neural network analysis. The geological factors used as inputs were S1 the mean SPT N value (standard penetration test) of the soil layers above crown level up to ground surface, S2 the average of the SPT N values at the crown, middle and invert levels, MC the average moisture content of the soil layer driven through by the tunnel machine, and E the average modulus of elasticity of the soil layer driven through by the tunnel machine. As the depth of the groundwater table did not vary significantly in

Table 2 Statistical summary of training and testing data

	min	max	ave	stdev
Cover H (m)	8.5	30	17.5	4.3
Advance rate AR (mm/min)	9.5	52.1	30.8	10.9
Earth pressure EP (kPa)	11	370	193.6	81.5
Mean SPT above crown level S1 (blows/300 mm)	0.66	80.33	27.9	28.2
Mean tunnel SPT S2 (blows/300 mm)	0	100	57.0	41.8
Mean moisture content MC (%)	5.95	66.48	27.1	18.7
Mean soil elastic modulus E (MPa)	5	120	72.9	50.8
Grout pressure GP (kPa)	27.7	700	258.6	154.9
Surface settlement (mm)	0.2	98.5	13.6	17.0

Table 3 Typical testing data samples

H (m)	AR (mm/min)	EP (kPa)	S1 (blows/300 mm)	S2 (blows/300 mm)	MC (%)	E (MPa)	GP (kPa)	Settlement (mm)
16.4	32.8	233.2	2.71	4.21	57.57	8.09	39.4	24.2
17.3	23	338	4.4	14.59	30.07	20.07	300	19.7
12	46.3	171	11.67	78.67	16.47	101.78	344	1.2
12	47.5	173.7	9.44	75.47	16.09	97.34	326	1.3
11	43.9	162	7.68	68.62	15.4	93.56	328	1.1
20	33.3	178.9	39.04	100	12.32	120	330	4.1
21	32	180.7	43.43	100	12.33	120	283	6
19.4	28	196	51.02	88.68	13.9	120	350	2.4
17.7	30	338	2.81	25.56	18.36	37.48	350	7.8
29	14.9	142.6	73	100	10.55	120	317	2.2
17.2	22	316	4.27	14.9	35.42	23.02	400	16.3
14.9	35	330	3.88	23.04	19.28	29.25	400	15.5
17.9	24	230	77.39	100	16.3	120	500	1.1
14.4	24	340	3.7	16.23	58.8	35.94	400	20.1
17.7	26	240	60.4	99.76	14.25	120	500	0.9
17.8	21	190	58.87	100	13.6	120	400	1.2
28	12.4	116.3	78.03	100	11.32	120	306	3.8
15.2	24	340	3.97	15.59	47.67	29.79	300	17.4

these three projects, it was omitted as one of the input parameters. The EPB operational factors used as inputs were AR the tunnel advance rate, EP the EPBM earth (face) pressure, and GP the grout pressure used for injecting grout into the tail void.

A total of 148 instrumented sections of settlement data (patterns) were obtained from the three projects. The ranges of the various parameters are shown in Table 2. A total of 115 sets of settlement data samples (patterns) were randomly selected as the training data and the remaining 33 data samples were used for testing the validity of the neural network. In this paper, a data sample refers to a set of input data and associated measured settlement corresponding to an instrumented section. Since for most practical cases, the serviceability limit is less than 30 mm, the testing

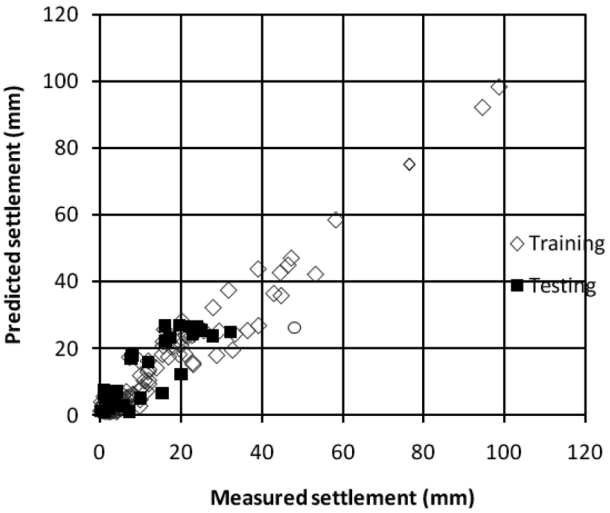

Fig. 6 Comparison of measured and predicted settlement values

samples that were less than 30 mm were randomly selected, while ensuring that the training and testing samples are statistically consistent. For brevity, only some of the testing samples are shown in Table 3.

The optimal neural network consisted of eight input neurons (H, AR, EP, S1, S2, MC, E and GP), five hidden neurons, and one output neuron representing the maximum surface settlement. The plots of the NN predicted versus the measured settlement values are shown in Fig. 6. The results indicated fairly high coefficient of correlation r between the actual and predicted settlement values of 0.9709 and 0.8642 for the training and testing samples, respectively. The root mean square error (Suwansawat and Einstein 2006) was 4.5 mm for the training samples and 5.2 mm for the testing samples. The mathematical expression for the trained network relating the input variables and the predicted surface settlement d_{NN} (output variable) is shown in the Appendix.

5. Reliability concepts

In civil engineering, reliability assessment may be cast essentially as a problem of "capacity" and "demand". For example, for a structure, in which the concern is to ensure that its strength (capacity) is sufficient to withstand the maximum applied load (demand) then the strength and load are modeled as random input variables and the outcome is a probability distribution of "failure" of the structure.

For a problem with multiple n random variables denoted by the vector $\mathbf{x}$, the calculation of the probability of "failure" involves the determination of a multi-dimensional joint probability density function (pdf) of the random variables, and the integration of the pdf over the failure domain $G(\mathbf{x})$. The hyper-surface $G(\mathbf{x}) = 0$ that separates the "failure" and "nonfailure" region in n-dimensional space is generally referred to as the limit state surface.

For multiple random variables such as this problem comprising eight input variables, the numerical integration of the pdf is computationally impractical. A well-developed approximate

alternative is to use the first-order reliability method (Hasofer and Lind 1974). Its popularity results from the mathematical simplicity of the method, since only second moment information (mean and standard deviation) on the random variables is required. The probability of failure is then assessed by the reliability index (Cornell 1969). Clear expositions of the underlying theory are found in various publications including Shinozuka (1983), Ang and Tang (1984), and Melchers (1987). Some examples of the use of the first order reliability method in geotechnical engineering have been presented by Low and Tang (2004), Goh and Kulhawy (2003) and Juang *et al.* (2006).

Mathematically, the reliability index (Ditlevsen 1981) is computed as

$$\beta = \min_{\mathbf{x} \in \mathrm{F}} \sqrt{(\mathbf{x}-\mathbf{m})^{\mathrm{T}} \mathbf{C}^{-1} (\mathbf{x}-\mathbf{m})} \tag{1}$$

or, equivalently (Low and Tang 2004)

$$\beta = \min_{\mathbf{x} \in \mathrm{F}} \sqrt{\left[\frac{\mathbf{x}-\mathbf{m}}{\sigma}\right]^{\mathrm{T}} \mathbf{R}^{-1} \left[\frac{\mathbf{x}-\mathbf{m}}{\sigma}\right]} \tag{2}$$

in which $\mathbf{x}$ is the vector representing the n random variables, $\mathbf{m}$ is the vector of the mean values of the random variables, σ is the standard deviation, $\mathbf{C}$ is the covariance matrix of the random variables, $\mathbf{R}$ is the correlation matrix, and F is the failure region. The minimization in Eq. (1) or Eq. (2) is performed over the failure domain F corresponding to the region $G(\mathbf{x}) < 0$. Low and Tang (2004) have shown that a spreadsheet environment can be used to perform the minimization and determine β. If the random variables have probability distributions close to normal, then the probability of failure P_f can be obtained from the expression

$$P_f \approx \Phi(-\beta) \tag{3}$$

in which $\Phi(-\beta)$ is the value of the cumulative probability. This value can be obtained from tables of the standard cumulative normal distribution function found in many textbooks or from built-in functions in most spreadsheets.

The first-order reliability method outlined above is equally applicable to non-normal and/or correlated variables. For non-normal probability distributions, this involves a transformation to the equivalent normal distribution. For correlated variables, this involves transforming the correlated variables to a set of uncorrelated variables for the correlation matrix $\mathbf{R}$ in Eq. (2) by finding the eigen-values and eigen-vectors. These procedures are detailed in Ang and Tang (1984).

In many situations such as in the modeling of surface settlement, the serviceability limit state surface is difficult to determine explicitly in terms of the random variable with simple polynomial functions. As an alternative, in this paper the neural network model described earlier is used to determine the limit state surface. Goh and Kulhawy (2003, 2005) have demonstrated the feasibility of integrating the neural network derived serviceability limit state surface for tunnels and braced excavation systems with reliability analysis in a spreadsheet environment. In this paper, the serviceability limit state or 'failure' is interpreted in the most general sense of unsatisfactorily performance when the predicted surface settlement exceeds the limiting surface settlement δ_{Lim}.

6. Reliability analysis

The eight random variables H, AR, EP, S1, S2, MC, E and GP are assumed to be lognormally distributed and uncorrelated. To illustrate the reliability analysis, two examples are presented. The mean values of the variables for these two examples are shown in Table 4. Case 1 corresponds to a soft layer of soil above the tunnel crown (S1 = 3) and stiffer soil in the tunnel (S2 = 30) while in the case 2, the soils above the tunnel crown and in the tunnel are assumed to be stiff. In the reliability analyses, it is assumed in these two examples that the limiting surface settlement δ_{Lim} is 30 mm. The selected 30 mm settlement value adopted here is for illustrative purposes only. The procedure outlined in this paper is valid for the evaluation of the probability of occurrence of a maximum surface settlement value, but not to building damage. Also, the coefficient of variation (COV) of the variables is assumed to be 0.2 except for H where a more realistic (for mass rapid transit tunnels with fixed alignments) and smaller COV of 0.05 was adopted. For simplicity and illustrative purposes, the variables are assumed to be non-correlated. As mentioned in the previous section, analysis for correlated variables can be carried out through transforming the correlated variables to a set of uncorrelated variables for the correlation matrix **R** in Eq. (2) by finding the eigen-values and eigen-vectors. These procedures are detailed in Ang and Tang (1984).

From the reliability analyses the probability P_f of δ_{Lim} being exceeded is determined, and the P_f values are shown in the last row of Table 4. The results indicate that P_f is very small for case 2 where the predicted settlement is 4.1 mm. For case 1 with a larger predicted settlement of 16.8 mm, a fairly high P_f of 26.8% was obtained.

With this integrated neural network-reliability approach it is possible to carry out sensitivity studies to examine the effect of the level of uncertainty of each parameter uncertainty (COV) on the probability of failure. Fig. 7 shows the significant influence of the mean value of AR on P_f (assuming the mean values and COV of the other variables, and the COV of AR are unchanged) for case 1. The effects of assuming the variables were normally distributed instead of lognormally distributed are also shown in Fig. 7. The results indicate the differences in P_f are minimal. Fig. 8 shows the effects of the COV of AR, GP and MC on P_f for case 1. The plots in Fig. 8 indicate that COV of the tunnel advance rate is the most critical factor that affects the P_f. Studies can also be carried out to evaluate the influence of δ_{Lim} on P_f as shown in Fig. 9.

Table 4 Parameters for case 1 and case 2

	Case 1	Case 2
H (m)	17	22
AR (mm/min)	30	48
EP (kPa)	350	235
S1 (blows/300 mm)	3	52
S2 (blows/300 mm)	30	100
MC (%)	20	18
E (MPa)	40	120
GP (kPa)	500	300
Settlement (mm)	16.8	4.1
P_f	0.267641	5.37×10^{-6}

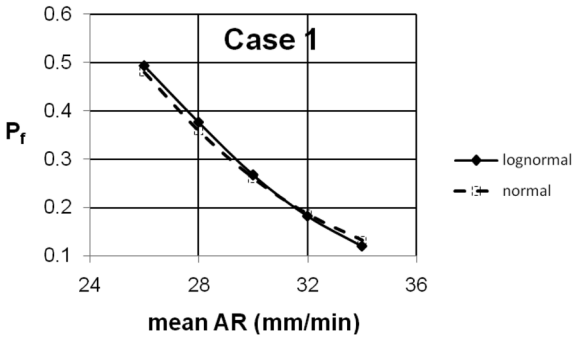

Fig. 7 Effects of mean values of AR on P_f for case 1

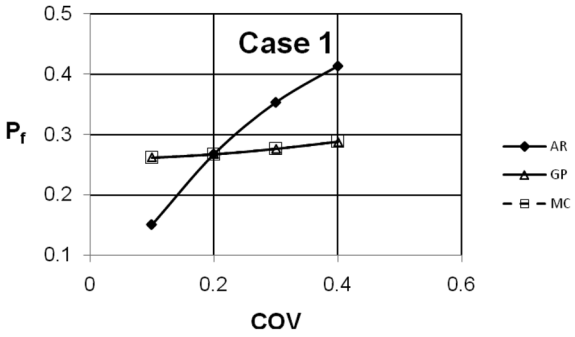

Fig. 8 Effects of COV of AR, GP and MC on P_f for case 1

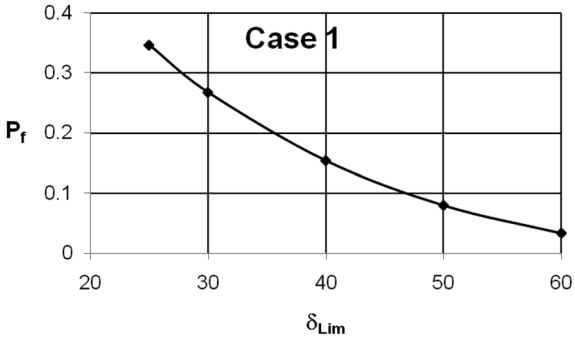

Fig. 9 Effects of δ_{Lim} on P_f for case 1

6. Conclusions

Predicting surface settlement for EPB tunnel operations is a highly nonlinear problem involving a number of input variables that include the geological conditions and the tunnel operation factors. Based on field measured data from three separate projects in Singapore, a neural network-reliability based design methodology has been developed through which uncertainties in the tunnel operation and geological parameters can be modeled and systematically analyzed. With this method, it is possible to carry out sensitivity studies to examine the effect of the level of uncertainty of each parameter uncertainty (COV) on the probability that the serviceability limit state has been exceeded.

Acknowledgements

The authors would like to thank Hon Hoy Seetoh, Nick Osborne and Khor Eng Leong from the Land Transport Authority for their invaluable assistance during the tunnel data collection which was undertaken by Dhony Hidayat.

References

Ang, A.H.S. and Tang, W.H. (1984), *Probability concepts in engineering planning and design*, Vol. II - Decision, risk and reliability, New York, John Wiley and Sons.

Attewell, P.B. (1977), "Ground movements caused by tunneling in soil", *Proc. Conf. on large ground movements and structures*, Pentech Press, London, 812-948.

Caudill, M. and Butler, C. (1991), *Naturally intelligent systems*, Cambridge MA, MIT Press.

Cornell, C.A. (1969), "A probability-based structural code", *ACI J.*, **66**(12), 974-985.

Ditlevsen, O. (1981), *Uncertainty modeling: with applications to multidimensional civil engineering systems*, New York, McGraw-Hill.

Goh, A.T.C. and Kulhawy, F.H. (2003), "Neural network approach to model the limit state surface for reliability analysis", *Can. Geotech. J.*, **40**(6), 1235-1244.

Goh, A.T.C. and Kulhawy, F.H. (2005), "Reliability assessment of serviceability performance of braced retaining walls using a neural network approach", *Int. J. Numer. Anal. Met.*, **29**(6), 627-642.

Hasofer, A.M. and Lind, N. (1974), "An exact and invariant first-order reliability format", *J. Eng. Mech.* - ASCE, **100**(1), 111-121.

Hornik, K. (1991), "Approximation capabilities of multilayer feedforward networks", *Neural Networks*, **4**(2), 251-257.

Hulme, T.W. and Burchell, A.J. (1999), "Tunneling projects in Singapore: an overview", *Tunn. Undergr. Sp. Tech*., **14**(4), 409-418.

Izumi, C., Khatri, N.N., Norrish, A. and Davies, R. (2000), "Stability and settlement due to bored tunneling for LTA, NEL", *Proc. Int. Conf. on tunnels and underground structures*, Singapore, 555-560.

Juang, C.H., Fang, S.Y. and Khor, E.H. (2006), "First-order reliability method for probabilistic liquefaction triggering analysis using CPT", *J. Geotech. Geoenviron. Eng.* - ASCE, **132**(3), 337-350.

Kim, C.Y., Bae, G.J., Hong, S.W., Park, C.H., Moon, H.K. and Shin, H.S. (2001), "Neural network based prediction of ground settlements due to tunneling", *Comput. Geotech.*, **28**(6-7), 517-547.

Low, B.K. and Tang, W.H. (2004), "Reliability analysis using object-oriented constrained optimization", *Struct. Safety*, **26**(1), 69-89.

Mair, R.J., Taylor, R.N. and Bracegirdle, A. (1993), "Subsurface settlement profiles above tunnels in clays", *Geotech.*, **43**(2), 315-320.

Melchers, R.E. (1987), *Structural reliability: analysis and prediction*, Chichester UK, Ellis Horwood Ltd.

Rowe, R.K. and Lee, K.M. (1992), "An evaluation of simplified techniques for estimating three dimensional undrained ground movements due to tunneling in soft soils", *Can. Geotech. J.*, **29**, 39-52.

Rumelhart, D.E., Hinton, G.E. and Williams, R.J. (1986), "Learning internal representation by error propagation", *Parallel distributed processing*, *Edited by* D.E. Rumelhart, J.L. McClelland, Cambridge MA, MIT Press, 318-362.

Santos, O.J. Jr. and Celestino, T.B. (2008), "Artificial neural networks of Sao Paulo subway tunnel settlement data", *Tunn. Undergr. Sp. Tech.*, **23**, 481-491.

Sharma, J.S., Chu, J. and Zhao, J. (1999), "Geological and geotechnical features of Singapore: an overview", *Tunn. Undergr. Sp. Tech.*, **14**(4), 419-431.

Shi, J., Ortigao, J.A.R. and Bai, J. (1998), "Modular neural networks for predicting settlements during tunneling", *J. Geotech. Geoenviron. Eng.* - ASCE, **124**(5), 389-395.

Shinozuka, M. (1983), "Basic analysis of structural safety", *J. Struct. Div.* - ASCE, **3**(109), 721-740.

Shirlaw, N., Ong, J.C.W., Rosser, H.B., Tan, C.G., Osborne, N.H. and Heslop, P.E. (2003), "Local settlements and sinkholes due to EPB tunneling", *Proc. ICE, Geotech. Eng.*, **156**(GE4), 193-211.

Suwansawat, S. and Einstein, H.H. (2008), "Artificial neural networks for predicting the maximum surface settlement caused by EPB shield tunneling", *Tunn. Undergr. Sp. Tech.*, **21**(2), 133-150.

Uriel, A.O. and Sagaseta, C. (1989), "Selection of design parameters for underground construction", *Proc. 12th ICSMFE*, Rio de Janeiro, Brazil, Balkema **4**, 2521-2551.

CC

Appendix

Calculation of settlement δ_{NN} using trained neural network

From the connection weights for a trained neuron network, it is possible to develop a mathematical equation relating the input parameters and the single output parameter Y using

$$Y = f_{sig}\left\{ b_o + \sum_{k=1}^{h} \left[w_k . f_{sig}\left(b_{hk} + \sum_{i=1}^{m} w_{ik} X_i \right) \right] \right\} \tag{3}$$

in which b_o is the bias at the output layer, w_k is the weight connection between neuron k of the hidden layer and the single output neuron, b_{hk} is the bias at neuron k of the hidden layer ($k = 1, h$), w_{ik} is the weight connection between input variable i ($i = 1, m$) and neuron k of the hidden layer, X_i is the input parameter i, and f_{sig} is the sigmoid (logistic) transfer function.

All inputs are scaled so that they correspond to roughly the same scale. Commonly chosen ranges are 0 to 1 or –1 to 1. In this paper, the following linear scaling equation was used

$$x_{\text{norm}} = 2\frac{x_{\text{actual}} - x_{\text{min}}}{x_{\text{max}} - x_{\text{min}}} - 1 \tag{4}$$

in which x_{norm} is the normalized input value, x_{actual} is the actual input value, x_{max} is the maximum value for x in the database, and x_{min} is the minimum value for x in the database.

Using the connection weights of the trained neural network, the following steps can be followed to calculate the surface settlement δ_{NN}:

Step 1: Normalize the eight input values for H, AR, EP, S1, S2, MC, E and GP linearly using Eq. (4) and the respective minimum and maximum values given in Table 2. Let the normalized input values be X1, X2, X3, X4, X5, X6, X7 and X8, respectively.

Step 2: Calculate the normalized deflection (Y1) using the following expressions

$$A1 = -0.6049485 - 1.647059X1 - 0.2618749X2 - 0.7239116X3 + 1.795338X4 + 2.323643X5 - 1.535398X6 + 2.75273X7 + 0.4491026X8 \tag{5}$$

$$A2 = 4.558665 + 0.09153855X1 + 3.070534X2 - 1.430003X3 - 1.16995X4 + 1.031811X5 + 0.3414552X6 + 0.4290629X7 + 3.030559X8 \tag{6}$$

$$A3 = -1.400228 + 1.933478X1 + 1.965984X2 + 0.462021X3 - 1.083987X4 - 1.462418X5 - 1.076024X6 - 0.6723999X7 + 0.6261287X8 \tag{7}$$

$$A4 = 0.8321956 + 0.9886981X1 + 0.1441506X2 - 0.2953318X3 + 0.1487119X4 + 0.5369028X5 - 4.266462X6 + 0.9782275X7 - 0.1734556X8 \tag{8}$$

$$A5 = -0.06946912 - 1.3320579X1 - 3.390786X2 - 0.4914406X3 - 0.486794X4 + 2.595912X5 - 1.280449X6 + 2.54284X7 - 0.5407983X8 \tag{9}$$

$$B1 = -2.626956/[1 + \exp(-A1)] \tag{10}$$

$$B2 = -3.574269/[1 + \exp(-A2)] \tag{11}$$

$$B3 = 2.481771/[1 + \exp(-A3)] \tag{12}$$

$$B4 = -1.768369/[1 + \exp(-A4)] \tag{13}$$

$$B5 = 4.862653/[1 + \exp(-A5)] \tag{14}$$

$$C1 = 0.9188275 + B1 + B2 + B3 + B4 \tag{15}$$

$$Y1 = 1/[1 + \exp(-C1)] \tag{16}$$

Step 3: De-normalize the output to obtain the settlement (units of mm)

$$\text{settlement } \delta_{NN} = 0.2 + 98.3(Y1 - 0.1)/0.8 \tag{17}$$